

Structural Determinants of Cisplatin and Transplatin Binding to the Met-Rich Motif of Ctr1: A Computational Spectroscopy Approach

Trung Hai Nguyen,^{†,||} Fabio Arnesano,^{‡,||} Simone Scintilla,[‡] Giulia Rossetti,[†] Emilio Ippoliti,[†] Paolo Carloni,^{*,†,§} and Giovanni Natile^{*,‡}

[†]Computational Biophysics, German Research School for Simulation Sciences, D-52425 Jülich, Germany, and Institute for Advanced Simulation, Forschungszentrum Jülich, D-52425 Jülich, Germany

[‡]Department Farmaco-Chimico, University of Bari “A. Moro”, via Edoardo Orabona 4, 70125 Bari, Italy

[§]Statistical and Biological Physics Sector, Scuola Internazionale Superiore di Studi Avanzati (SISSA), Via Bonomea 265, I-34136 Trieste, Italy

Supporting Information

ABSTRACT: The cellular uptake of cisplatin and of other platinum-based drugs is mediated by the high-affinity copper transporter Ctr1. The eight-residue long peptide called Mets7 (MTGMKGMS) mimics one of extracellular methionine (Met)-rich motifs of Ctr1. It is an excellent model for investigating the interaction of platinum drugs with Ctr1 under in vitro and in vivo conditions. Some of us have shown that (i) Cisplatin loses all of its ligands upon reaction with Mets7 and the metal ion binds to the three Met residues and completes its coordination shell with a fourth ligand that can be a chloride or a water/hydroxyl oxygen. (ii) Transplatin loses only the chlorido ligands, which are replaced by Met residues. Here, we provide information on the structural determinants of cisplatin/Mets7 and transplatin/Mets7 adducts by computational methods. The predictions are validated against EXAFS, NMR, and CD spectra. While EXAFS gives information restricted to the metal coordination shell, NMR provides information extended to residue atoms around the coordination shell, and finally, CD provides information about the overall conformation of the peptide. This allows us to elucidate the different reaction modes of cisplatin and transplatin toward the peptide, as well as to propose the platinated peptides $[PtX]^{+}-(M^{*}TGM^{*}KGM^{*}S)$ ($X = Cl^{-}, OH^{-}$) and $trans[Pt(NH_3)_2]^{2+}-(M^{*}TGM^{*}KGM^{*}S)$ as the most relevant species occurring in water solution.

I. INTRODUCTION

Cisplatin [*cis*-diamminedichloridoplatinum(II)] is one of the most widely used anticancer drugs. It is active against many types of cancer, such as testicular, ovarian, cervical, and colorectal cancers and relapsed lymphoma.^{1,2} Unfortunately, the drug suffers from several drawbacks, such as side effects and intrinsic or acquired resistance, which severely limit the efficacy of the drug.¹ The cellular mechanisms behind the resistance to cisplatin and other platinum-based drugs are multifactorial and not completely understood.³ The generally accepted mechanism involves an increased cisplatin detoxification, an improved repair of the DNA lesions, and a decreased accumulation of the drug.³ Among these factors, the reduced drug accumulation is a common and distinctive feature of resistant cells.⁴ It is, therefore, important to characterize the molecular mechanisms of cisplatin's efflux and cellular uptake. The first involves the copper pumps ATP7A and ATP7B in the secretory vesicles⁵ and the cytosolic copper chaperone Atox1. All of these proteins can bind cisplatin and enhance its efflux/sequestration.⁶ Cisplatin may be also ensnared in melanosomes that are subsequently exported from the cells.⁷ The cellular uptake is governed, at least in part, by the homotrimeric copper transporter Ctr1.^{3,8} Ctr1 forms a channel-like pore in the membrane,⁹ featuring intra- and extracellular domains. Flow of the active platinum substrate through the channel-like pore of the Ctr1 trimer has been proposed.^{10,11} Alternatively, cisplatin could form coordination bonds with the protein. The

extracellular N-terminal domain contains methionine(Met)-rich motifs, which are able to bind copper.¹² Met sulfur is indeed a good donor atom for platinum.¹³ Hence, some cisplatin could bind to the extracellular Met-rich motifs of Ctr1 and an endocytic vesicle might be formed. In this way the vesicle could incorporate cisplatin present in the extracellular solution while protecting the drug from deactivation and transporting it to subcellular compartments.^{14,15} To provide insights on Ctr1–cisplatin interactions, some of us have carried out in vitro studies on reactions of cisplatin, the inactive isomer transplatin (*trans*-diamminedichloridoplatinum(II)), and other platinum complexes with the MTGMKGMS peptide (Mets7).^{14,15} The latter mimics the seventh Met-rich motif of yeast Ctr1. Circular dichroism (CD) measurements showed that Mets7 features a β -turn conformation after reacting with cisplatin, while it is a random coil in the Apo form.¹⁴ Furthermore, electrospray mass spectrometry (ESI-MS) data showed that cisplatin progressively loses all ammine and chlorido ligands and ultimately coordinates only to Mets7.¹⁶ Consistently, 1H and ^{13}C nuclei of $\epsilon\text{-CH}_3$ and $\gamma\text{-CH}_2$ of methionines feature a large downfield shift in NMR spectra upon platinum coordination.¹⁴ Other groups reported a similar binding mode of cisplatin to partial or full-length N-terminal domain of human Ctr1.^{19,20} Hence, Mets7 is a good mimic of

Received: February 28, 2012

Published: June 18, 2012



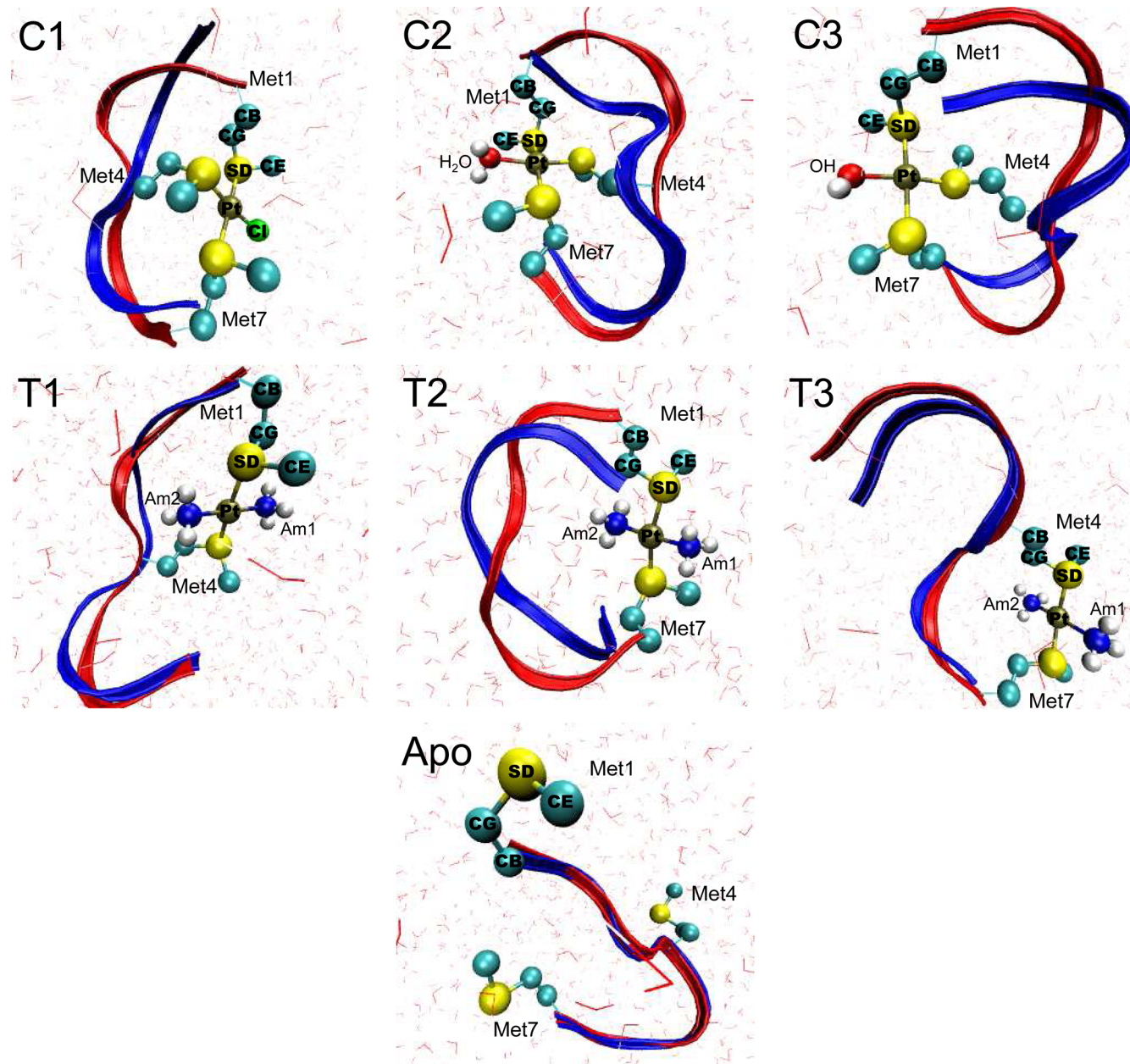


Figure 1. Structural models of platinated and Apo peptides emerging from REST and QM/MM simulations. The backbone conformations of the last QM/MM snapshot (in red ribbons) and a representative REST snapshot (in blue ribbons) are superimposed. The QM atoms are shown in stick-and-balls ($\text{CB} \equiv \text{C}_\beta$, $\text{CG} \equiv \text{C}_\gamma$, $\text{CE} \equiv \text{C}_\epsilon$). Water is shown in lines. Counterions are not shown for the sake of clarity.

the N-terminal domains of Ctr1 in terms of reactivity against cisplatin.

The structural basis of cisplatin and transplatin binding to Mets7 is still lacking. Herein, we have addressed this issue by using computational tools. Simulation approaches are indeed widely used to investigate cisplatin and its interactions with biomolecules.^{21–39} Specifically, we have used hybrid Car-Parrinello density functional theory-based QM/MM simulations^{40–43} on models of platinated Mets7, extracted from available experimental information.¹⁴ We have already used this approach for platinated DNA.^{44–46} These models contain the platinum moieties ($[\text{PtCl}]^+$, $[\text{Pt}(\text{H}_2\text{O})]^{2+}$, $[\text{Pt}(\text{OH})]^+$, and $\text{trans-}[\text{Pt}(\text{NH}_3)_2]^{2+}$). The QM/MM simulations, albeit rather accurate, can cover only rather short time scales (0.1 ns or less). While these are likely to be enough to provide valuable information on the local platinum coordination, global

conformational properties of the peptide are out of reach. To extend the time scale of the simulations, we have developed AMBER-type⁵⁵ force field parameters of the platinum moieties based on the QM/MM simulations via the so-called “force matching” procedure.⁴⁷ The parameters are derived so as to reproduce the QM/MM forces, the electrostatic potential, and the electric field obtained by QM/MM simulations, as already done for platinated DNA in ref 48. Finally, 0.2- μs -long replica exchange simulations based on these force field parameters for the metal coordination shell and on AMBER parm99SB^{55,56} for the biomolecular frame are performed for the platinated peptide as well as for the unbound peptide. The accuracy of the predicted models is established by a comparison with the NMR and CD data already reported in the literature,¹⁴ as well as EXAFS spectra measured expressly for this study.

II. METHODS

Computational Chemistry. Mets7 (Apo hereafter) was built as a linear chain by using the Leap package.⁴⁹ In the cisplatin/Mets7 adducts (C1–C3, Figure 1), the platinum coordination was taken from DFT-based optimized model compounds (section 1, Table S1, Supporting Information), with the Mets7's three methionine sulfurs and either a chloride (C1), or a water oxygen (C2), or a hydroxyl oxygen (C3) acting as donor atoms. In the transplatin/Mets7 adducts (T1–T3, Figure 1), the donor atoms are two ammine nitrogens and two sulfur atoms of either Met1 and Met4 (T1), or Met1 and Met7 (T2), or Met4 and Met7 (T3). The six systems, along with Apo, were inserted in boxes containing water molecules and chloride counterions (Table S2, Supporting Information).

The platinated and Apo peptides were subjected to 0.4 μ s of preparatory AMBER-based molecular dynamics (MD) simulations using the NAMD program (see section 2, Supporting Information for details).⁵⁰ A cluster analysis⁵¹ allowed us to identify representative structures of the most populated clusters. It turned out that only one cluster was sufficient to comprise 70% or more of the conformational space explored by the MD trajectories. Hence, we considered only the representatives of the most populated clusters.

The six representative structures of C1–C3 and T1–T3 underwent hybrid Car–Parrinello QM/MM simulations.^{52,40–43} We used the CPMD program⁵³ combined with the classical MD GROMOS96 code,⁵⁴ through the interface developed by Rothlisberger et al.⁴¹ The MM regions comprised the peptide frame, the solvent, and the counterions (Figure 1). These were described with the AMBER parm99SB force field⁵⁵ with the “Stony Brook” modification for the backbone torsions,⁵⁶ the TIP3P model for the solvent,⁵⁷ and the Smith and Dang force field for the counterions.⁵⁸ The QM part concerns the platinum coordination polyhedron (Figure 1) and was treated by density functional theory (DFT), with the BLYP recipe for the exchange–correlation functional.^{59,60} The wave function was expanded in a plane-wave basis setup to an energy cutoff of 70 Ry. Only the valence electrons were treated explicitly (in the case of Pt, electrons in the $n = 5$ shell are also included in the valence). The core electrons were described using norm-conserving pseudopotentials of the Martins–Troullier type.⁶¹ Isolated system conditions were applied.⁶² The β carbon (CB) atoms linked to the MM part by covalent bonds were saturated by “capping” hydrogen atoms.⁴² The electrostatic interactions between QM and MM atoms were calculated using a fully Hamiltonian hierarchical scheme.⁴¹ In particular, the short-range electrostatic interactions between QM and MM part were taken explicitly into account within a radius of 5.3 Å around every QM atom using an appropriate modified Coulomb potential to prevent electron spill-out.⁴¹ Beyond this first shell and within 10.6 Å, the electrostatic interactions are calculated using the D-RESP charge scheme.⁴⁰ In the outermost region, a multipole expansion scheme is used.⁴¹ A time step of 0.097 fs was used. A fictitious electronic mass of 400 au for the Car–Parrinello dynamics was employed. Constant temperature conditions were achieved using the Nosé–Hoover chain thermostat.^{63–65} Nonbonded interactions were evaluated as in the previous MD simulations. A total of 2000 steps of simulated annealing were performed to relax the representative snapshots of the previous MD simulations. Then, the systems were slowly heated up to 300 K by gradually

increasing the target temperature (30 K after every 1000 steps). Finally, 25-ps-long QM/MM simulations were carried out.

AMBER-type force field parameters of the QM regions were obtained by applying the force matching procedure of refs 47 and 48 to 300 QM/MM conformations, selected every 0.08 ps. The atomic partial charges (Tables S5 and S6, Supporting Information) were obtained through a fit to the electrostatic potential and the electric field. These, along with van der Waals parameters taken from AMBER parm99SB force field,^{55,66} were subtracted from the total forces acting on the QM atoms to yield the bonded forces. A least-squares fit of the latter allowed us to obtain the AMBER-type bond, angle, and dihedral angle force field parameters. Equilibrium bond lengths and bond angles were taken from the QM/MM averaged values. The parameters for Met, water, and OH turned out to differ only by 30–40% relative to the original AMBER parameters.

Apo, C1–C3, and T1–T3 underwent, respectively, 0.5, 0.2, and 0.2 μ s replica exchange with solute tempering (REST) simulations⁶⁷ in the NPT ensemble (see section 3, Supporting Information for more details).⁶⁸ Eight replicas covered a temperature range from 300 to 600 K for each system (Figure S4, Supporting Information). The force field was the same as that of the previous MD simulations except that the platinated moieties were described by the parameters obtained via the force matching procedure. First, each replica was prepared independently by 5-ns-long MD simulations, and then the REST simulations were performed with the replica exchange being attempted after every 5 ps. The acceptance ratios were between 15 and 25%. The integration step of 2 fs was used. In each replica, the temperature was controlled by Nosé–Hoover chain thermostat,^{63–65} whereas the pressure was controlled by Parrinello–Rahman barostat.⁶⁹ The REST simulations were carried out with the Gromacs 4.5.3 program.⁷⁰ The DSSP approach^{71,72} was used to assign the secondary structures to the conformations along each of the REST trajectories. The percentage of each secondary structure type was then estimated from the frequency of its occurrence during the REST simulations. The CD spectra were averaged values over 500 equidistant snapshots along the 200-ns-long REST trajectories. The web interface DichroCalc^{73,74} was used. The CD spectra turned out not to change with increasing REST simulation time (Figure S5, Supporting Information), suggesting that these calculated properties are well-converged during the simulations.

Next, 25-ps-long QM/MM simulations were carried out for Apo starting from the representative structures obtained from REST simulation. The QM part of the Apo model includes three Met residues (Figure 1). The MM part consists of the peptide frame, the solvent, and the counterions. Exactly the same procedure as the one carried out for the platinated peptides was employed. Finally, the last snapshots of the REST trajectories of Apo, C1–C3, and T1–T3 underwent 25-ps-long QM/MM simulations with the same QM/MM procedure described above.

NMR and EXAFS spectra were evaluated on the basis of the QM/MM simulations of Apo and the platinated peptides before and after the REST calculations. The results of the first and the latter are reported in the Supporting Information and in the main text, respectively. ^1H , ^{13}C , and ^{195}Pt NMR shielding constants were calculated as averages over the 50 equidistant QM/MM snapshots. For the first two nuclei, we used the approach in refs 75 and 76 for the QM parts of C1–C3, T1–T3, and Apo. They were converted to the NMR chemical shifts using the shielding constant of tetramethylsilane (TMS) as in

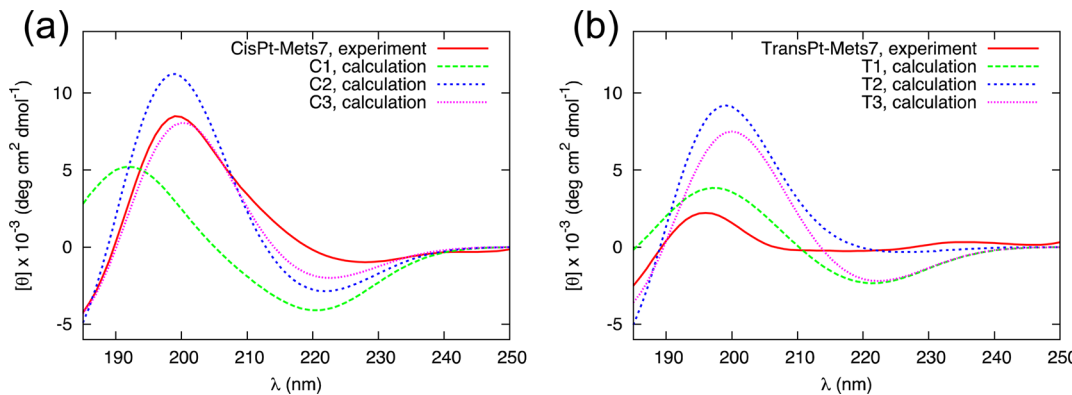


Figure 2. Calculated and experimentally measured¹⁴ CD spectra of cisplatin/Mets7 (a) and transplatin/Mets7 (b) adducts.

ref 77 (for more details, see section 4, Supporting Information).⁷⁸ For ¹⁹⁵Pt NMR shielding constants we used the ADF code^{79–81} on the QM parts of C1–C3 and of T1–T3. The quadruple- ζ quadruply polarized basis set QZ4P for the Pt and the triple- ζ singly polarized basis set TZP for the other atoms were used. The calculations were carried out at the DFT-PBE level.⁸² This choice of basis sets and functional was shown to give reliable results for the calculation of ¹⁹⁵Pt chemical shifts.⁸³ Scalar relativistic effects were taken into account with the zero-order regular approximation (ZORA) approach.^{84,85} The MM atoms were included as point charges. The chemical shift was referenced to that of $[\text{PtCl}_6]^{2-}$ in water at room temperature, as obtained by an additional QM/MM simulation (see section 5, Supporting Information, for details).

The EXAFS spectra were calculated at the Pt edge. The FEFF6L code^{86–88} was applied over 500 equidistant QM/MM snapshots.⁸⁹ For each snapshot, a cluster of atoms within 5 Å from the platinum atom was extracted, taking into account the periodic boundary conditions, and input into the FEFF6L program to generate the EXAFS spectrum. The k^3 -weighted EXAFS spectra were Fourier-transformed using the IFEFFIT program⁹⁰ to obtain the real-space representation.

EXAFS Measurements. The samples were prepared as follows: 3.0 mM aqueous solutions of Apo containing 100 mM NaCl were treated with one mol equiv of either cisplatin or transplatin and the mixtures were kept for 24 h at 310 K before recording the XAS spectra. The adduct formation between Mets7 and the selected platinum complex was checked by ESI-MS as previously described.¹² The samples were loaded in Teflon cells with Kapton windows, mounted in a two-stage Displex cryostat, and kept at 20 K during the data collection. XAS spectra were recorded at beamline D2 of the European Molecular Biology Laboratory (EMBL) outstation at Deutsches Elektronen Synchrotron (DESY, Hamburg, Germany). The DORIS storage ring operated at 4.5 GeV with the positron beam current ranging from 150 to 95 mA. Ionization chambers in front and behind the sample were used to monitor the beam intensity. A Si(111) double-crystal monochromator scanned X-ray energies around the platinum L₃-edge (11 564 eV). The X-ray absorption spectra were recorded as platinum L₃ fluorescence spectra with a Canberra 13-element germanium solid-state detector. For both samples, 10 scans were collected and averaged to ensure comparable statistics. Data reduction, such as background removal, normalization, and extraction of the fine structure, was performed with KEMP.⁹¹ The extracted platinum L³-edge extended X-ray absorption fine structure (EXAFS) data were converted to photoelectron wave vector k

space and weighted by k^3 . The full, k^3 -weighted EXAFS spectra (30–1000 eV above E_0) and their Fourier transforms (FT) calculated over the range 2.0–16.0 Å⁻¹ were compared with theoretical simulations.

III. RESULTS AND DISCUSSION

In the cisplatin/Mets7 adducts (C1–C3, Figure 1), the three methionine sulfurs act as donor atom to the Pt(II) ion, while the remaining fourth position may be occupied by chloride (C1), water molecule (C2), or hydroxyl group (C3). In the transplatin/Mets7 adducts (T1–T3), the two ammine ligands remain bound to Pt in trans arrangement. The other two ligands come from the two methionine sulfurs of either Met1,4 (T1), Met1,7 (T2) or Met4,7 (T3).

After having developed a force field for the platinated moiety using the force matching approach (see Methods), we used replica exchange with a solute tempering (REST) method and subsequent QM/MM simulations to investigate the Pt(II) ion coordination and the conformational properties of these platinated peptides, along with the conformational feature of the unbound peptide (Apo, Figure 1). The direct comparison between the calculated and experimental spectroscopic data (EXAFS from this work, along with NMR and CD from ref 14) established the accuracy of our structural predictions.

Peptide Conformation. During the QM/MM simulations, the peptides' conformations do not change significantly (rmsd between the first and the last snapshot <0.8 Å). The structures obtained from REST simulations are not too dissimilar to those from QM/MM simulations (Figure 1): The averaged rmsd of REST structures with respect to the last QM/MM snapshots ranges from 1.1 to 2.2 Å (Table S10, Supporting Information). The C1–C3 models are less flexible than the T1–T3 ones, as indicated by an analysis of the RMSF values. These are less than 1 Å for the first and between 1.1 and 1.6 Å for the latter (Table S11, Supporting Information). The content of the secondary structure (ss) during the REST simulations is given in Table S12, Supporting Information.

In the case of cisplatin/Mets7 adducts, C2 and C3 contain more β -turn (>47%) than coil (<38%). In contrast, C1 contains more coil (50%) than β -turn (30%), and a small content of α -helix (8%). In the case of transplatin/Mets7, T1 contains mostly coil (59%) and only 26% of β -turn. Instead, both T2 and T3 have more β -turn than coil. Bends are found in all cases with rather small content (<16%). In the models with large β -turn contents, the latter is more likely to be found between the platinated methionines. The large content of turn appears to

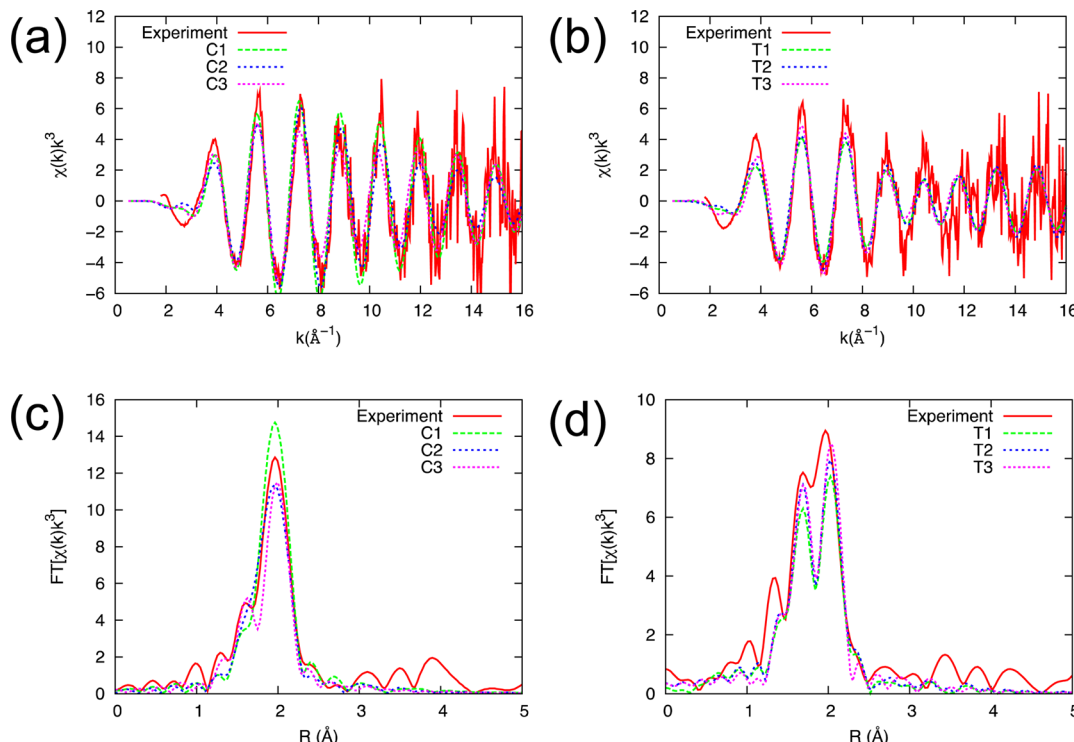


Figure 3. Calculated and experimental EXAFS spectra at the Pt edge of cisplatin/Mets7 (a) and transplatin/Mets7 (b) adducts. The experimental spectrum has been measured in this work. Fourier transforms of the spectra in panels a and b are given in panels c and d, respectively. They are plotted as a function of the scattering path length of the photoelectron, R . Note that R does not correspond to a real interatomic distance since the peak positions are shifted inward, with respect to the bond distances, due to the phase shifts of the photoelectron (i.e., increase in its kinetic energy caused by the electronic potentials of both the scattering and the absorbing atoms).⁹⁸ The shift, therefore, depends on both the absorbing and scattering atom types, and in our cases is approximately 0.4 Å (Table S3, Supporting Information).

correlate with the emerging β -turn-type band in the calculated CD spectrum (Figure 2).

CD Spectra. The calculated CD spectrum of C3 is in good agreement with the experimental one (Figure 2a). It has a positive peak at 200 nm, which features the β -turn conformation.⁹² The CD spectrum of the C2 model has a similar shape, but its intensity is slightly larger than that of the experimental spectrum. In contrast, in the spectrum of C1, the positive peak is shifted toward a lower wavelength (\sim 190 nm) compared to the experimental peak. In addition, it features a weak negative band at \sim 210 nm. Hence, C2 and C3 reproduce better the β -turn feature of the experimental CD spectrum than C1. Since the only difference between C2 and C3 is the state of deprotonation of the coordinated solvent molecule (Figure 1), an equilibrium between the two species may be present.

The calculated CD spectrum of T1 reproduces fairly well the experimental one (Figure 2b). Those of T2 and T3 have a very large positive band at about 200 nm, which features their β -turn conformation. This contrasts with the experimental observation that the binding of transplatin to Mets7 only slightly modifies the random coil structure of the free peptide.¹⁴ This might imply that only T1 gives an important contribution to the total CD spectrum of the transplatin/Mets7 adduct, while T2 and T3 are almost irrelevant. The calculated CD spectrum of Apo has a positive band at \sim 195 nm and a negative band at \sim 210 nm, which suggest some content of β sheet structure. However, the experimental spectrum is characteristic of a random coil conformation.¹⁴ The reason behind the discrepancy between experiment and theory might be due to sampling issues and to limitation of the force field. In particular, simulations based on

the AMBER force field,^{55,56} which has been used here, might bias random coiled structures toward the formation of secondary structure elements.^{93–96} In this respect, we stress here that the main focus of the paper is to reproduce the structural determinants of the platinated peptides, for which our computational procedure appears to be quite accurate.

Platinum Coordination. In the QM/MM simulations, the Pt geometry deviates only slightly from the ideal square-planar geometry, e.g., the difference from a square angle is less than 10% (Table S3, Supporting Information). The Pt–S bond lengths range from 2.3 to 2.4 Å (Table S3, Supporting Information). These values are very similar to those of corresponding model compounds ($[\text{Pt}(\text{SH}_2)_3\text{Cl}]^+$, $[\text{Pt}-(\text{SH}_2)_3\text{H}_2\text{O}]^{2+}$, $[\text{Pt}(\text{SH}_2)_3\text{OH}]^+$, and *trans*- $[\text{Pt}-(\text{SH}_2)_2(\text{NH}_3)_2]^{2+}$) optimized in the gas phase (Table S1, Supporting Information). Oxygen atoms from water molecules and/or the peptide terminus occupy the axial positions of the platinum complex, at a distance from the metal ranging from 2.6 to 2.8 Å (Figure S3, Supporting Information). In the REST simulations, the bond lengths and angles are very similar to those of QM/MM simulations (Table S3, Supporting Information).

From the QM/MM calculations, local spectral properties can also be obtained. Despite the short time scale, the QM/MM calculations can provide rather accurate spectroscopic properties of the Pt site. This is because the overall conformations of the peptides, and in particular of the Pt site, in the QM/MM simulations are not too dissimilar to those obtained by the subsequent sampling-enhanced REST simulations. Further-

Table 1. ^{13}C (top) and ^1H (bottom) NMR Chemical Shifts (in ppm) of the Pt-Coordinated Met Residues of Cisplatin/Mets7 (C1–C3) and Transplatin/Mets7 (T1–T3) Adducts after REST Simulations^a

Met no.	atom name	^{13}C NMR							experimental values		
		calculated values							Apo	cisplatin/Mets7	transplatin/Mets7
		Apo	C1	C2	C3	T1	T2	T3			
Met1	C_γ	31.1 (3.5)	35.7 (5.8)	37.2 (5.2)	39.3 (4.9)	33.9 (4.1)	39.5 (4.9)		29.3	34.1	34.3
	C_ε	17.3 (2.3)	21.3 (4.9)	21.6 (3.0)	23.3 (2.8)	22.2 (2.7)	20.5 (5.1)		14.2	19.9	18.5
Met4	C_γ	30.4 (2.4)	40.4 (5.2)	40.3 (5.6)	39.2 (5.2)	37.9 (4.3)		38.8 (5.6)	29.3	34.1	34.3
	C_ε	17.2 (2.5)	18.5 (4.0)	21.5 (3.2)	21.6 (2.1)	15.9 (3.1)		21.2 (3.8)	14.2	19.9	18.5
Met7	C_γ	32.3 (2.6)	39.5 (5.9)	39.6 (5.2)	37.2 (5.4)		40.2 (5.3)	39.1 (5.8)	29.3	34.1	34.3
	C_ε	16.9 (2.7)	17.5 (4.1)	18.0 (4.2)	15.8 (3.7)		21.1 (4.5)	21.0 (3.4)	14.2	19.9	18.5
^1H NMR											
Met No.	atom name	calculated values							experimental values		
		Apo	C1	C2	C3	T1	T2	T3	Apo	cisplatin/Mets7	transplatin/Mets7
	H_γ	2.65 (0.45)	2.78 (0.36)	2.84 (0.35)	3.18 (0.44)	3.52 (0.34)	3.12 (0.36)		2.51	2.89	3.03
Met4	H_ε	2.41 (0.26)	2.60 (0.43)	2.62 (0.42)	2.71 (0.41)	2.76 (0.27)	2.79 (0.42)		2.03	2.35	2.51
	H_γ	2.70 (0.40)	2.90 (0.51)	3.05 (0.53)	3.02 (0.39)	3.47 (0.27)		3.61 (0.45)	2.51	2.89	3.03
Met7	H_ε	2.24 (0.37)	2.61 (0.50)	2.57 (0.52)	2.44 (0.49)	2.54 (0.29)		2.62 (0.30)	2.03	2.35	2.51
	H_γ	2.64 (0.34)	3.36 (0.59)	3.21 (0.53)	3.03 (0.52)		3.68 (0.45)	3.32 (0.40)	2.51	2.89	3.03
	H_ε	2.45 (0.38)	2.79 (0.59)	2.66 (0.37)	2.63 (0.61)		2.56 (0.33)	2.62 (0.38)	2.03	2.35	2.51

^aThe corresponding values before REST simulations are reported in Tables S13–S15 (Supporting Information). Standard deviations are shown in parentheses. See Figure 1 for atom name conventions.

more, the QM region is relatively well sampled within the QM/MM time scale (see section 6, Supporting Information).

EXAFS Spectra. The calculated k^3 -weighted EXAFS spectra at the Pt edge of C1–C3 and T1–T3 reproduce well the experimental data (Figure 3a,b). Also the corresponding Fourier transforms (FT's) of the calculated EXAFS spectra are in fair agreement with those of the experiments (Figure 3c,d).

For the cisplatin/Mets7 adducts (Figure 3c) the three FT's feature a large peak, mainly caused by the backscattering from the three Pt-bound sulfur atoms and a chloride (C1) or a water oxygen (C2); a small side peak on the left which appears clearly only in C3 is due to the hydroxyl oxygen (see section 7, Supporting Information, for the assignment of peaks to the corresponding ligand's atoms).⁹⁷ The main contributions from each type of ligand's atoms to the total EXAFS spectra are shown in Figure S2 (Supporting Information). The peak heights of C2 and C3 are lower than the experimental one. On the contrary, the peak height of C1 is greater. We note that the EXAFS spectra were taken at high chloride concentration (100 mM, see Methods), while the CD spectra were taken at low chloride concentration (see ref 14). Therefore, model C1, which did not appear to give significant contribution to the CD spectrum, could give a significant contribution to the EXAFS spectrum.

For the transplatin/Mets7 adducts (Figure 3d), the FT's feature two large distinct peaks in the first coordination shell. The first peak is due to the ammine nitrogen atoms and the second peak is due to the Met sulfur atoms (Figure S2, Supporting Information). The large difference in length between Pt–S and Pt–N bonds (Table S3, Supporting Information) causes such a splitting.⁹⁷ The magnitude of FT's of T1–T3 is slightly smaller than those obtained by experiment.

NMR Spectra. The calculated ^{13}C and ^1H NMR chemical shifts of the platinated and Apo peptides reproduce the experimental values within the indicated standard deviations (Table 1). In particular, as observed for the experimental data,

the values of ^1H and ^{13}C chemical shifts at the $\gamma\text{-CH}_2$ and $\varepsilon\text{-CH}_3$ residues of the platinated peptides (C1–C3 and T1–T3) are larger than those of the Apo (Table 1). This is consistent with the experimental observation that the binding of cisplatin and transplatin to the Mets7 peptide causes a large downfield shift in the NMR signals for the $\gamma\text{-CH}_2$ and $\varepsilon\text{-CH}_3$ atoms of all three methionines.¹⁴ The downfield shift of $\gamma\text{-CH}_2$ and $\varepsilon\text{-CH}_3$ atoms of all three methionines, also in the case of the transplatin/Mets7 adducts where only two methionines are coordinated to platinum, indicates that the three models are in fast exchange, even if they can contribute differently to the overall spectrum.

The calculated ^{195}Pt chemical shifts of C1 and C3 reproduce quite well the experimental data (Table 2). That of C2 deviates

Table 2. ^{195}Pt NMR Chemical Shifts (in ppm) of the Cisplatin/Mets7 (C1–C3) and Transplatin/Mets7 (T1–T3) Adducts after REST Simulations^a

Cisplatin/Mets7		Transplatin/Mets7	
model	chemical shifts	model	chemical shifts
experiment	−4100	experiment	−2900
C1	−3815 (321)	T1	−2793 (353)
C2	−2793 (361)	T2	−3121 (347)
C3	−3571 (382)	T3	−2751 (286)

^aThe corresponding values before REST simulations are reported in Table S16, (Supporting Information). Standard deviations are shown in parentheses.

significantly from the experimental value. This might imply that the C2 model is less relevant than C1 and C3. As already pointed out in the discussion of the EXAFS spectra, also the NMR spectra were taken at a rather high chloride concentration (3.0 mM). Under these conditions model C1 could gain relevance and contribute to the overall NMR spectra. The ^{195}Pt NMR chemical shifts of T1–T3 do not differ very much. The difference between cisplatin/Mets7 and

transplatin/Mets7 (\sim 1000 ppm) is fairly well reproduced by our calculations.

The use of the REST trajectories for calculating the CD spectra, rather than the QM/MM trajectories that have been used to calculate the NMR and EXAFS spectra, deserve an additional comment. The CD spectrum is obviously sensitive to the global conformations of the peptides' backbone. Therefore, we used for its calculation a sampling-enhanced technique, such as REST,⁶⁷ that samples extensively the conformational space. On the other hand, the NMR chemical shifts of the Pt ligands and the EXAFS spectra at the Pt edge are expected to be sensitive to the local geometry (bond lengths and bond angles) of the platinum coordination shell. QM/MM describes accurately the metal ion coordination polyhedra in metal-based biomolecules.⁴² Therefore, we can expect accurate results based on the QM/MM trajectories. However, in this case sampling is obviously much more limited than in the case of the REST simulations. To address this issue, we compare the results from two sets of QM/MM calculations, before (Tables S13–S14, Supporting Information) and after (Tables 1–2) the REST simulations. It turns out that the results are essentially the same, in spite of the fact that the conformations of the peptide frame at the end of the REST trajectories are rather different from those at the beginning. On the basis of these findings, we suggest that the EXAFS and NMR shifts do not depend significantly on the peptides' global conformations but rather they depend on the local environment. This feature has been found also in several other bioinorganic systems.^{99–101}

IV. CONCLUSIONS

The cellular uptake of cisplatin is mediated by the high-affinity copper transporter Ctr1.^{3,8} The eight-residue-long peptide (Mets7) is able to mimic the extracellular Met-rich N-terminal motifs of yeast Ctr1.¹⁴ The reaction of cisplatin and transplatin with Mets7 was characterized experimentally by some of us.¹⁴ Here, the structural and spectroscopic properties of cisplatin and transplatin adducts with Mets7 (models C1–C3 and T1–T3, respectively; see Figure 1) have been investigated, for the first time, by hybrid Car–Parrinello QM/MM simulations. Information about the overall conformation of the peptide could be deduced from CD spectra. To this end, 200-ns-long REST simulations were carried out for the adduct models. The simulations were based on the force field parameters obtained by force matching procedure⁴⁷ for the platinated moieties. The configurationally averaged CD spectra were calculated for each of the models.

It turns out that the CD spectra of different simulated species show rather different patterns. As for the CD spectrum of the cisplatin/Met7 adduct, we notice that the band wavelengths of the spectra of C2 and C3 models is characteristic of a β -turn structure. This is in a good agreement with the experimental one. In detail, the spectrum of C3 matches the intensity of the experimental one better than that of C2. In contrast, C1 model shows much worse correspondence, particularly in terms of band wavelengths. We conclude that (i) the spectrum of the C3 model, in which the ligands of the Pt(II) ion are three Met residues and a hydroxyl group, gives the most important contribution to the total CD. In addition, (ii) in the experimental conditions of ref 14, the coordinated water molecule is deprotonated so as to reduce the net positive charge of the complex. In the case of the transplatin/Mets7 CD spectrum, the band intensities and wavelengths of the T1 model show good agreement with the experimental ones.

Those of the T2 and T3 models are instead significantly different from the experimental ones and show a strong signal characteristic of a β -turn structure. We conclude that the T1 model (coordination to platinum of Met1 and Met4, Figure 1) is likely to give a much greater contribution to the total CD than those of the other two models.

Concerning the Pt coordination, since experimental data for the bond lengths and angles are not available, the consistency between the Pt-coordination geometry of the simulated models and the real ones has been checked by comparing the calculated Pt EXAFS spectra of C1–C3 and T1–T3 with the experimental ones reported here for the first time. The calculated EXAFS spectra of the three models show good agreement with the experimental spectra. Differently from the CD spectra, the EXAFS spectra were taken at considerably higher chloride concentration. Hence, model C1 (chlorido species), which did not contribute appreciably to the CD spectra, can instead give a significant contribution to the EXAFS spectra. Calculations show that, indeed, this is the case.

The calculated ^1H and ^{13}C NMR chemical shifts are in rather good agreement with the experimental chemical shifts. The differences in the calculated ^1H and ^{13}C NMR chemical shifts between Apo and platinated peptides confirm that platinum binding causes a downfield shift of the NMR signals belonging to the Met residues that are bound to platinum as observed experimentally. The calculations also confirm a contribution of models T2 and T3 to the overall spectra to account for the downfield shift observed for $\gamma\text{-CH}_2$ and $\varepsilon\text{-CH}_3$ of all methionines of Mets7. The calculated ^{195}Pt chemical shifts also show that model C1 can give a relevant contribution to the experimental spectrum taken at a rather high chloride concentration. In contrast, model C2, whose computed spectrum significantly deviates from the experimental one, contributes much less.

Different spectroscopies, combined with quantum chemical calculations, provide valuable complementary insights in bioinorganic systems.¹⁰² Here, we have calculated a variety of spectroscopic data (CD, EXAFS, and NMR), which are readily compared with experiments. The exhaustive comparison of the calculated spectroscopic data with the experimental ones has been proved useful. It allows us to make structural prediction of platinated Mets7 species in aqueous solution. The full QM/MM and REST trajectories of all the complexes are freely available upon request to the authors.

ASSOCIATED CONTENT

S Supporting Information

Supporting methods; structural data of gas-phase-optimized model compounds, QM/MM, and REST structures; the cosine content of the principal components of the QM region; force field parameters obtained from the force matching procedure; averaged backbone RMSDs of REST structures with respect to last QM/MM structures; the root-mean-square fluctuations (RMSF) of REST trajectories; secondary structure contents of REST trajectories; comparison of NMR before and after REST calculations; RMSDs of QM zone in QM/MM simulations; contributions from each type of scattering atoms to the total EXAFS spectra; Pt–O radial pair distribution; potential energy distribution of replicas in REST simulations; running average of CD spectra and ^{195}Pt NMR chemical shifts; and comparison of EXAFS before and after REST simulations. This information is available free of charge via the Internet at <http://pubs.acs.org/>.

AUTHOR INFORMATION

Corresponding Author

*E-mail: natile@farmchim.uniba.it (G.N.), p.carloni@grs-sim.de (P.C.).

Author Contributions

[†]These authors contributed equally.

Notes

The authors declare no competing financial interest.

ACKNOWLEDGMENTS

This work was funded by the Italian Ministero dell'Università e della Ricerca (MIUR-PRIN 2008.R23Z7K), Deutsche Forschungsgemeinschaft (CA 973/8-1), and Contributi ex art. 23 L.R.26/2005-Progetto NANOCANCER "Nuove strategie nanotecnologiche antitumorali". The authors thank the University of Bari, the Consorzio Interuniversitario di Ricerca in Chimica dei Metalli nei Sistemi Biologici (CIRCMSB), the European Commission (COST Actions CM0902 and CM1105) for support and the EMBL Hamburg Outstation for providing access to synchrotron radiation beamline. We gratefully acknowledge Prof. Elena Borghi and Dr. Wolfram Meyer-Klaucke for assistance in EXAFS measurements. We thank Dr. Francesco Musiani for his assistance in the REST simulations and Dr. Alessandro Marchiori for useful discussions. Computer time provided by the Jülich Supercomputing Center on JUROPA is gratefully acknowledged.

REFERENCES

- (1) Andrews, P. A.; Howell, S. B. *Cancer Cells* **1990**, *2*, 35–43.
- (2) Kelland, L. *Nat. Rev. Cancer* **2007**, *7*, 573–584.
- (3) Hall, M. D.; Okabe, M.; Shen, D. W.; Liang, X. J.; Gottesman, M. M. *Annu. Rev. Pharmacol. Toxicol.* **2008**, *48*, 495–535.
- (4) Safaei, R.; Howell, S. B. *Crit. Rev. Oncol. Hematol.* **2005**, *53*, 13–23.
- (5) Dolgov, N. V.; Olson, D.; Lutsenko, S.; Dmitriev, O. Y. *Biochem. J.* **2009**, *419*, 51–56.
- (6) Arnesano, F.; Banci, L.; Bertini, I.; Felli, I. C.; Losacco, M.; Natile, G. *J. Am. Chem. Soc.* **2011**, *133*, 18361–18369.
- (7) Chen, K. G.; Valencia, J. C.; Lai, B.; Zhang, G.; Paterson, J. K.; Rouzaud, F.; Berens, W.; Wincoffitch, S. M.; Garfield, S. H.; Leapman, R. D.; Hearing, V. J.; Gottesman, M. M. *Proc. Natl. Acad. Sci. U. S. A.* **2006**, *103*, 9903–9907.
- (8) Ishida, S.; Lee, J.; Thiele, D. J.; Herskowitz, I. *Proc. Natl. Acad. Sci. U. S. A.* **2002**, *99*, 14298–14302.
- (9) Aller, S. G.; Unger, V. M. *Proc. Natl. Acad. Sci. U. S. A.* **2006**, *103*, 3627–3632.
- (10) Larson, C. A.; Adams, P. L.; Jandial, D. D.; Blair, B. G.; Safaei, R.; Howell, S. B. *Biochem. Pharmacol.* **2010**, *80*, 448–454.
- (11) Wang, X.; Du, X.; Li, H.; Chan, D. S.; Sun, H. *Angew. Chem., Int. Ed. Engl.* **2011**, *50*, 2706–2711.
- (12) Puig, S.; Lee, J.; Lau, M.; Thiele, D. J. *J. Biol. Chem.* **2002**, *277*, 26021–26030.
- (13) Wang, X.; Guo, Z. *Anti-Cancer Agents Med. Chem.* **2007**, *7*, 19–34.
- (14) Arnesano, F.; Scintilla, S.; Natile, G. *Angew. Chem., Int. Ed. Engl.* **2007**, *46*, 9062–9064.
- (15) Arnesano, F.; Natile, G. *Pure Appl. Chem.* **2008**, *80*, 2715–2725.
- (16) Since it is believed that cisplatin has to keep the two ammine ligands to be active,^{17,18} the observation that cisplatin loses all ligands by interacting with the extracellular domain of Ctrl might have important implications for the mechanism of cellular uptake of cisplatin promoted by this transporter.^{14,15}
- (17) Brabec, V. *Prog. Nucleic Acid Res. Mol. Biol.* **2002**, *71*, 1–68.
- (18) Todd, R. C.; Lippard, S. J. *Metallomics* **2009**, *1*, 280–291.
- (19) Wu, Z.; Liu, Q.; Liang, X.; Yang, X.; Wang, N.; Wang, X.; Sun, H.; Lu, Y.; Guo, Z. *J. Biol. Inorg. Chem.* **2009**, *14*, 1313–1323.
- (20) Crider, S. E.; Holbrook, R. J.; Franz, K. J. *Metallomics* **2010**, *2*, 74–83.
- (21) Lopes, J. F.; Rocha, W. R.; Dos Santos, H. F.; De Almeida, W. B. *J. Chem. Phys.* **2008**, *128*, 165103–165116.
- (22) Chen, J. C.; Chen, L. M.; Liao, S. Y.; Zheng, K. C.; Ji, L. N. *Phys. Chem. Chem. Phys.* **2009**, *11*, 3401–3410.
- (23) Wu, Y.; Bhattacharyya, D.; King, C. L.; Baskerville-Abraham, I.; Huh, S. H.; Boysen, G.; Swenberg, J. A.; Temple, B.; Campbell, S. L.; Chaney, S. G. *Biochemistry* **2007**, *46*, 6477–6487.
- (24) Deubel, D. V. *J. Am. Chem. Soc.* **2002**, *124*, 5834–5842.
- (25) Sutter, K.; Truflandier, L. A.; Autschbach, J. *ChemPhysChem* **2011**, *12*, 1448–1455.
- (26) Truflandier, L. A.; Sutter, K.; Autschbach, J. *Inorg. Chem.* **2011**, *50*, 1723–1732.
- (27) Lau, J. K.; Ensing, B. *Phys. Chem. Chem. Phys.* **2010**, *12*, 10348–10355.
- (28) Fu, C. F.; Tian, S. X. *J. Chem. Phys.* **2010**, *132*, 174507–174513.
- (29) Téletchéa, S.; Skauge, T.; Sletten, E.; Kozelka, J. *Chemistry* **2009**, *15*, 12320–12337.
- (30) Springer, A.; Bürgel, C.; Böhrsch, V.; Mitrić, R.; Bonacić-Koutecký, V.; Linscheid, M. W. *ChemPhysChem* **2006**, *7*, 1779–1785.
- (31) Scheeff, E. D.; Briggs, J. M.; Howell, S. B. *Mol. Pharmacol.* **1999**, *56*, 633–643.
- (32) Dans, P. D.; Coitiño, E. L. *J. Chem. Inf. Model.* **2009**, *49*, 1407–1419.
- (33) Zimmermann, T.; Chval, Z.; Burda, J. V. *J. Phys. Chem. B.* **2009**, *113*, 3139–3150.
- (34) Baik, M. H.; Friesner, R. A.; Lippard, S. J. *J. Am. Chem. Soc.* **2002**, *124*, 4495–4503.
- (35) Zhang, Y.; Guo, Z.; You, X. Z. *J. Am. Chem. Soc.* **2001**, *123*, 9378–9387.
- (36) Zimmermann, T.; Zeizinger, M.; Burda, J. V. *J. Inorg. Biochem.* **2005**, *99*, 2184–2196.
- (37) Matsui, T.; Shigeta, Y.; Hirao, K. *J. Phys. Chem. B.* **2007**, *111*, 1176–1181.
- (38) Deubel, D. V. *J. Am. Chem. Soc.* **2004**, *126*, 5999–6004.
- (39) Monjardet-Bas, V.; Elizondo-Riojas, M. A.; Chottard, J. C.; Kozelka, J. *Angew. Chem., Int. Ed. Engl.* **2002**, *41*, 2998–3001.
- (40) Laio, A.; VandeVondele, J.; Rothlisberger, U. *J. Phys. Chem. B* **2002**, *106*, 7300–7307.
- (41) Laio, A.; VandeVondele, J.; Rothlisberger, U. *J. Chem. Phys.* **2002**, *116*, 6941–6947.
- (42) Rothlisberger, U.; Carloni, P. Simulations of enzymatic systems: Perspectives from Car–Parrinello molecular dynamics simulations. In *Theoretical Biochemistry: Processes and Properties of Biological Systems*, 1st ed.; Politzer, P., Maksic, Z. B., Eds.; Elsevier Science: Amsterdam, The Netherlands, 2001; Vol. 9, pp 215–251.
- (43) Dal Peraro, M.; Ruggerone, P.; Raugei, S.; Gervasio, F. L.; Carloni, P. *Curr. Opin. Struct. Biol.* **2007**, *17*, 149–156.
- (44) Spiegel, K.; Rothlisberger, U.; Carloni, P. *J. Phys. Chem. B* **2004**, *108*, 2699–2707.
- (45) Magistrato, A.; Ruggerone, P.; Spiegel, K.; Carloni, P.; Reedijk, J. *J. Phys. Chem. B* **2006**, *110*, 3604–3613.
- (46) Spiegel, K.; Magistrato, A. *Org. Biomol. Chem.* **2006**, *4*, 2507–2517.
- (47) Maurer, P.; Laio, A.; Hugosson, H. W.; Colombo, M. C.; Rothlisberger, U. *J. Chem. Theory Comput.* **2007**, *3*, 628–639.
- (48) Spiegel, K.; Magistrato, A.; Maurer, P.; Ruggerone, P.; Rothlisberger, U.; Carloni, P.; Reedijk, J.; Klein, M. L. *J. Comput. Chem.* **2008**, *29*, 38–49.
- (49) Zhang, W.; Hou, T.; Schafmeister, C.; Ross, W. S.; Case, D. A. *LEaP and gleap, AmberTools User's Manual*, Ver. 1.5, 2011.
- (50) Phillips, J. C.; Braun, R.; Wang, W.; Gumbart, J.; Tajkhorshid, E.; Villa, E.; Chipot, C.; Skeel, R. D.; Kalé, L.; Schulten, K. *J. Comput. Chem.* **2005**, *26*, 1781–1802.
- (51) Micheletti, C.; Seno, F.; Maritan, A. *Proteins* **2000**, *40*, 662–674.
- (52) Car, R.; Parrinello, M. *Phys. Rev. Lett.* **1985**, *55*, 2471–2474.

- (53) CPMD, version 3.15.1; IBM Corp. 1990–2008, MPI für Festkörperforschung Stuttgart 1997–2001; <http://www.cpmd.org> (accessed April 26, 2012).
- (54) van Gunsteren, W. F. *Biomolecular Simulation: The GROMOS96 Manual and User Guide*; Verlag der Fachvereine Hochschulverlag AG an der ETH Zurich: Zurich, 1996.
- (55) Wang, J.; Cieplak, P.; Kollman, P. A. *J. Comput. Chem.* **2000**, *21*, 1049–1074.
- (56) Hornak, V.; Abel, R.; Okur, A.; Strockbine, B.; Roitberg, A.; Simmerling, C. *Proteins* **2006**, *65*, 712–725.
- (57) Jorgensen, W. L.; Chandrasekhar, J.; Madura, J. D.; Impey, R. W.; Klein, M. L. *J. Chem. Phys.* **1983**, *79*, 926–935.
- (58) Smith, D. E.; Dang, L. X. *J. Chem. Phys.* **1994**, *100*, 3757–3766.
- (59) Becke, A. D. *Phys. Rev. A* **1988**, *38*, 3098–3100.
- (60) Lee, C.; Yang, W.; Parr, R. G. *Phys. Rev. B* **1988**, *37*, 785–789.
- (61) Troullier, N.; Martins, J. L. *Phys. Rev. B* **1991**, *43*, 1993–2006.
- (62) Martyna, G. J.; Tuckerman, M. E. *J. Chem. Phys.* **1999**, *110*, 2810–2821.
- (63) Nose, S. *J. Chem. Phys.* **1984**, *81*, 511–519.
- (64) Hoover, W. G. *Phys. Rev. A* **1985**, *31*, 1695–1697.
- (65) Martyna, G. J.; Klein, M. L.; Tuckerman, M. J. *Chem. Phys.* **1992**, *97*, 2635–2633.
- (66) Yao, S.; Plastaras, J. P.; Marzilli, L. G. *Inorg. Chem.* **1994**, *33*, 6061–6077.
- (67) Liu, P.; Kim, B.; Friesner, R. A.; Berne, B. J. *Proc. Natl. Acad. Sci. U. S. A.* **2005**, *102*, 13749–13754.
- (68) The initial structures of the platinumated peptides were the last QM/MM snapshots, while for Apo, the initial linear structure inserted in water was used.
- (69) Parrinello, M.; Rahman, A. *Phys. Rev. Lett.* **1980**, *45*, 1196–1199.
- (70) Hess, B.; Kutzner, C.; van der Spoel, D.; Lindahl, E. *J. Chem. Theory Comput.* **2008**, *4*, 435–447.
- (71) Kabsch, W.; Sander, C. *Biopolymers* **1983**, *22*, 2577–2637.
- (72) Joosten, R. P.; Te Beek, T. A. H.; Krieger, E.; Hekkelman, M. L.; Hooft, R. W. W.; Schneider, R.; Sander, C.; Vriend, G. *Nucleic Acids Res.* **2011**, *39*, D411–D419.
- (73) Bulheller, B. M.; Hirst, J. D. *Bioinformatics* **2009**, *25*, 539–540.
- (74) Besley, N. A.; Hirst, J. D. *J. Am. Chem. Soc.* **1999**, *121*, 9636–9644.
- (75) Putrino, A.; Sebastiani, D.; Parrinello, M. *J. Chem. Phys.* **2000**, *113*, 7102–7109.
- (76) Sebastiani, D.; Parrinello, M. *J. Phys. Chem. A* **2001**, *105*, 1951–1958.
- (77) Röhrig, U. F.; Sebastiani, D. *J. Phys. Chem. B* **2008**, *112*, 1267–1274.
- (78) Because the QM/MM boundary cuts through the CA–CB bonds, the CB and HB atoms are very close to the MM part. They are expected to be overpolarized by the nearby MM charges. Hence, the calculation of chemical shifts was not carried out for them.
- (79) te Velde, G.; Bickelhaupt, F. M.; Baerends, E. J.; Fonseca Guerra, C.; van Gisbergen, S. J. A.; Snijders, J. G.; Ziegler, T. *J. Comput. Chem.* **2001**, *22*, 931–967.
- (80) Fonseca Guerra, C.; Snijders, J. G.; te Velde, G.; Baerends, E. J. *Theor. Chem. Acc.* **1998**, *99*, 391–403.
- (81) ADF2010, SCM, *Theoretical Chemistry*; Vrije Universiteit, Amsterdam: The Netherlands; <http://www.scm.com> (accessed April 26, 2012).
- (82) Hammer, B.; Hansen, L. B.; Nørskov, J. K. *Phys. Rev. B* **1999**, *59*, 7413–7421.
- (83) Sterzel, M.; Autschbach, J. *Inorg. Chem.* **2006**, *45*, 3316–3324.
- (84) van Lenthe, E.; Baerends, E. J.; Snijders, J. G. *J. Chem. Phys.* **1993**, *99*, 4597–4610.
- (85) Wolff, S. K.; Ziegler, T.; van Lenthe, E.; Baerends, E. J. *J. Chem. Phys.* **1999**, *110*, 7689–7698.
- (86) Rehr, J. J.; Mustre de Leon, J.; Zabinsky, S. I.; Albers, R. C. *J. Am. Chem. Soc.* **1991**, *113*, 5135–5140.
- (87) Rehr, J. J.; Albers, R. C.; Zabinsky, S. I. *Phys. Rev. Lett.* **1992**, *69*, 3397–3400.
- (88) Rehr, J. J.; Albers, R. C. *Rev. Mod. Phys.* **2000**, *72*, 621–654.
- (89) The FEFF calculation of EXAFS spectra are cheaper than that of NMR chemical shifts. Therefore, a larger number of QM/MM snapshots were used for EXAFS calculations.
- (90) Newville, M.; Ravel, B.; Haskel, D.; Rehr, J. J.; Stern, E. A.; Jacoby, Y. *Physica B* **1995**, *208*, 154–156.
- (91) Korbas, M.; Marsa, D. F.; Meyer-Klaucke, W. *Rev. Sci. Instrum.* **2006**, *77*, 063105–063109.
- (92) Perczel, A.; Hollosi, M.; Foxman, B. M.; Fasman, G. D. *J. Am. Chem. Soc.* **1991**, *113*, 9772–9784.
- (93) Best, R. B.; Buchete, N.-V.; Hummer, G. *Biophys. J.* **2008**, *95*, L07–L09.
- (94) Thompson, E. J.; DePaul, A. J.; Patel, S. S.; Sorin, E. J. *PLoS One.* **2010**, *5*, e10056.
- (95) Best, R. B.; Hummer, G. *J. Phys. Chem. B* **2009**, *113*, 9004–9015.
- (96) Best, R. B.; Mittal, J. *J. Phys. Chem. B* **2010**, *114*, 8790–8798.
- (97) In all cases, oxygen atoms at the axial positions are found to give a small contribution to the EXAFS signals (Figure S2, Supporting Information).
- (98) Zabinsky, S. I.; Rehr, J. J.; Ankudinov, A.; Albers, R. C.; Eller, M. *J. Phys. Rev. B* **1995**, *52*, 2995–3009.
- (99) Machonkin, T. E.; Westler, W. M.; Markley, J. L. *Inorg. Chem.* **2005**, *44*, 779–797.
- (100) Liptak, M. D.; Wen, X.; Bren, K. L. *J. Am. Chem. Soc.* **2010**, *132*, 9753–9763.
- (101) Chan, J.; Merrifield, M. E.; Soldatov, A. V.; Stillman, M. J. *Inorg. Chem.* **2005**, *44*, 4923–4933.
- (102) Solomon, E. I. *Inorg. Chem.* **2006**, *45*, 8012–8025.